Scientific paper

Synthesis of Er- and Yb-doped Gadolinium Oxide Polymorphs and Influence of Their Structures on Upconversion Properties

Janez Križan,[1] Matjaž Mazaj,[2,*] Venčeslav Kaučič,[2,3] Ivan Bajsić[4] and Janez Možina[4]

[1] *AMI d.o.o., Trstenjakova 5, 2250 Ptuj, Slovenia*

[2] *National Institute of Chemistry, Hajdrihova 19, 1000 Ljubljana, Slovenia*

[3] *CO-NOT Centre of Excellence, Hajdrihova 19, 1000 Ljubljana, Slovenia*

[4] *University of Ljubljana, Faculty of Mechanical Engineering, Aškerčeva 6, 1000 Ljubljana, Slovenia*

** Corresponding author: E-mail: matjaz.mazaj@ki.si*

Received: 15-01-2014

Abstract

Nanocrystalline Gd_2O_3 products doped with Er^{3+} and Yb^{3+} cations were synthesized by combustion method. We showed that the temperature of combustion can be tuned by using different types of organic fuels within reaction mixture. The combustion process is performed at lower temperature in the presence of urea as an organic fuel leading to pure cubic Gd_2O_3:Er,Yb phase, on the other hand higher combustion temperature, yielding pure monoclinic Gd_2O_3:Er,Yb polymorph is achieved in the mixture of urea and β-alanine. Effective doping of Er^{3+} and Yb^{3+} cations within Gd_2O_3 were confirmed by XRD analysis. Both polymorphs show upconversion in green and red areas and possess strong dependence of fluorescence intensity ratios (I_{525}/I_{549} or I_{525}/I_{560} for monoclinic and cubic polymorphs, respectively) on temperature. This indicates that both phases can be applied for the temperature sensor devices based on upconversion intensity ratio changes.

Keywords: Upconversion, gadolinium oxide, fluorescence, Yb-doping, Er-doping

1. Introduction

Doped rare-earth oxide materials with luminiscent properties are widely explored for various applications such as the development of laser devices, temperature sensors and field emission displays.[1–4] The trend of technology miniaturization and employing to medical diagnostics requires the development of these materials in sub-micron dimensions while keeping the luminiscent properties comparable with those in monocrystal form or preferably improving them. Common synthesis procedures in order to obtain nanosized rare-earth oxides includes hydrothermal treatment, sol-gel procedures, precipitation or flame combustion.[5–8] Flame combustion process is most frequently used due to the simplicity and low cost of the synthesis procedures and also due to the possibility of tailoring the size and morphology of particles. Gadolinium oxide nanoparticles are promising single-phase multifunctional probes possessing both magnetic and optical properties within one nanoparticle.[9,10] Gd_2O_3 is also known to be an excellent host matrix for luminescent rare-earth ions to produce downconversion or upconversion phosphors which means the ability to emit visible or ultra-violet light with subsequent excitation with near-infra red radiation via multiphoton process.[11] Upconversion of light from infra-red to visible wavelength region in rare-earth oxides attracted much attention due to their potential use in IR converters and upconversion short wavelength solid-state lasers. The upconversion luminescent probes also have considerable advantage over the conventionally used fluorescent dyes and quantum dots since the autofluorescence effect is removed and signal-to-noise ratio is significantly improved.[12,13] Trivalent cation Er^{3+}, as a dopant, is a good can-

didate for upconversion, due to its multiple electronic energy states which enable long lifetimes of intermediate states resonant with near infra-red excitation light, however the relative low absorption cross section of this ion in the UV region gives poor emission efficiency.[14,15] The additional presence of Yb^{3+} enables efficient energy transfer from ytterbium to erbium cations and larger absorption cross section due to the large spectral overlap between Yb^{3+} emission of $^2F_{5/2} \rightarrow {}^2F_{7/2}$ and Er^{3+} absorption of $^4I_{11/2} \leftarrow {}^4I_{15/2}$. This can significantly improve the upconversion emission.[16–19]

In this contribution we describe the synthesis of Er- and Yb-doped Gd_2O_3 nanopowders prepared by combustion method using gadolinium nitrate and gadolinium oxide as precursors and urea or mixture of urea and beta alanine as fuels. We showed that with the use of different fuel types, the crystallization process of Gd_2O_3:Er,Yb can be easily tuned. The phase purity and nanoparticle morphologies were investigated by X-ray powder diffraction (XRD) and scanning electron microscopy (SEM). Synthesized materials show intensive upconversion and fluorescence in green area (520–570 nm) and the shape of upconversion spectra is strongly dependent on Gd_2O_3:Er,Yb structure. Additionally, we investigated the effect of heating on upconversion spectra under IR illumination. Obtained materials can be used as fluorescence thermometers where the temperature is detected on a basis of changes of absorption maxima intensities in fluorescent spectra.

2. Experimental

2. 1. Synthesis

All chemicals were commercially available and used in synthesis procedures without further purification. $Gd(NO_3)_3.6H_2O$, $Er(NO_3)_3.5H_2O$ and $Yb(NO_3)_3.5H_2O$ were purchased from ABCR, all having purity of 99.9% purity , Gd_2O_3 (99.9 %) from NOAH Technologies and HNO_3 (65%) urea and β-alanine from Sigma-Aldrich.

Monoclinic Gd_2O_3:Er,Yb. Ytterbium- and erbium-doped monoclinic Gd_2O_3 nanopowders were synthesized by flame combustion method. The dry mixture of 22.57 g (50 mmol) of $Gd(NO_3)_3.6H_2O$, 0.55 g (1.25 mmol) of $Er(NO_3)_3 \cdot 5H_2O$ and 0.11 g (0.25 mmol) of $Yb(NO_3)_3 \cdot 5H_2O$ was combined with the mixture of 1.56 g (17.5 mmol) of β-alanine and 8.26 g (137.5 mmol) of urea which were used as organic fuels. So prepared starting reagents were combusted with the flame burner at approximately 500 °C. Intensive exothermic reaction yielded voluminous foamy pink powder. In the second step the product was sintered at 1300 °C for 2 hours. Safety precautions should be followed (use of heat resistant gloves and safety glases) due to the intensive heat release in the first step of the synthesis.

Cubic Gd_2O_3:Er,Yb. Ytterbium- and erbium-doped cubic Gd_2O_3 nanopowders were synthesized similarly as monoclinic product by flame combustion method. 9.06 g (25 mmol) of Gd_2O_3, 0.55 g (1.25 mmol) of $Er(NO_3)_3 \cdot 5H_2O$, 0.11 g (0.25 mmol) of $Yb(NO_3)_3 \cdot 5H_2O$ and the excess of concentrated HNO_3 (9.6 ml, 150 mmol) were combined with 7.51 g (125 mmol) of urea, used as organic fuel. Starting reaction mixture was combusted with the flame burner at approximately 500 °C, yielding pink foamy powder as in the case of synthesis of monoclinic product. Note that flame pyrolisis reaction was less intensive in comparison with the combustion of mixture yielding monoclinic Gd_2O_3:Er,Yb product. Material was additionally sintered at 1300 °C for 2 hours.

Non-doped Gd_2O_3. Non-doped gadolinium oxide materials with monoclinic and cubic structures, used as references, were synthesized by identical procedures as Yb-, Er-doped analogues with an absence of ytterbium and erbium precursors.

2. 2. Characterization Methods

X-ray powder diffraction (XRD) patterns were recorded on a PANalytical X'Pert PRO high-resolution diffractometer with Alpha1 configuration using CuK_α radiation (1.5406 Å) in the range from 20 to 50 ° 2θ with the step 0.017 ° per 100 s using fully opened 100 channel X'Celerator detector. Scanning electron microscopy (SEM) was studied on a Zeiss Supra 3VP field-emission microscope operating at 1 kV. The upconversion spectra were recorded on an OceanOptics USB4000 spectrometer at excitation of 980 nm using diode-pumped solid-state (DPSS) laser light source with the power of 1.5 W. The length of illumination was 50 cm and the beam was focused into the 0.6 mm optical fiber with ilumination area of 2 × 3 mm. For monitoring temperature dependency of upconversion band intensities, the powdered products were spread on the surface of the ceramic temperature probe with ceramic glue. Fluorescence spectra were then measured at different temperatures with excitation wavelength of 980 nm.

3. Results and Discussion

3. 1. Structure Analysis

XRD pattern shown in Figure 1a indicates that Gd_2O_3:Er,Yb material in the presence of urea and β-alanine crystallized in monoclinic crystal system (*C2/m*) with high degree of crystallinity and purity. The absence of any additional peaks that could belong to Yb_2O_3 or Er_2O_3 phases is the first evidence of efficient doping of Er^{3+} and Yb^{3+} cations into Gd_2O_3 without phase segregation. At first impression the presence of Er^{3+} and Yb^{3+} dopants does not affect the crystal structure of Gd_2O_3. Ho-

wever, close inspection and comparison of first few reflections with the reflections of non-doped Gd_2O_3 indicates that in XRD pattern of as-synthesized monoclinic Gd_2O_3:Er,Yb those peaks are slightly shifted towards higher angles in respect with non-doped Gd_2O_3 (Figure 1b). Shifting of the reflections towards higher angles is another proof of effective doping of Er^{3+} and Yb^{3+} within Gd_2O_3 and it is related to the unit cell contraction due to the smaller ionic radii of Er^{3+} and Yb^{3+} dopants (0.881 Å and 0.858 Å, respectively) in comparison with radius of Gd^{3+} (0.938 Å). The Table 1 show *d*-values which correspond to the 2θ positions of three selected reflections of non-doped monoclinic Gd_2O_3 and as-synthesized monoclinic Gd_2O_3:Er,Yb and their corresponding unit cell dimensions, obtained by TREOR package and refined by Rietveld method. The XRD reflections of sintered monoclinic Gd_2O_3:Er,Yb are at the same 2θ positions as in the pattern of as-synthesized product which indicates that subsequent sintering process at 1300 °C does not additionally affect the unit cell dimension. Scanning electron micrograph (SEM) of as-synthesized monoclinic Gd_2O_3:Er,Yb shown on Figure 2a reveals the presence of individual nanoparticles with the estimated size of 50 nm which are densely agglomerated into the foamy texture. The observed average particle size is in agreement with the calculated values obtained by Scherrer equation (77 nm). Sintering process does not notably improve the crystallinity, as can be indicated by XRD patterns, but it leads to significant increase of particle size up to 1 μm, due to the merging of individual nanoparticles to larger crystallites (Figure 2b).

Synthesis of Gd_2O_3:Er,Yb in the presence of only urea used as an organic fuel yields phase pure Gd_2O_3 with cubic crystal system (*Ia-3*) as can be seen in Figure 3. Interestingly, the presence of dopants significantly increases the degree of crystallinity in comparison with pure Gd_2O_3. Similarly as in the case of doping in monoclinic Gd_2O_3, the presence of Er^{3+} and Yb^{3+} cations within cubic Gd_2O_3 structure affect the unit cell dimension as indicated by the slight shift of the 2θ positions in XRD pattern of cubic Gd_2O_3:Er,Yb in respect with non-doped Gd_2O_3 (Table 1). SEM micrograph of as-synthesized cubic Gd_2O_3:Er,Yb shown in Figure 4a reveals that nanoparticles with the estimated size up to 250 nm are agglomerated into foamy texture possessing interparticle porosity. The particle size determined by Scherrer calculations was 220 nm. In contrast to monoclinic polymorph, the size of cubic Gd_2O_3:Er,Yb particles after sintering process at 1300 °C

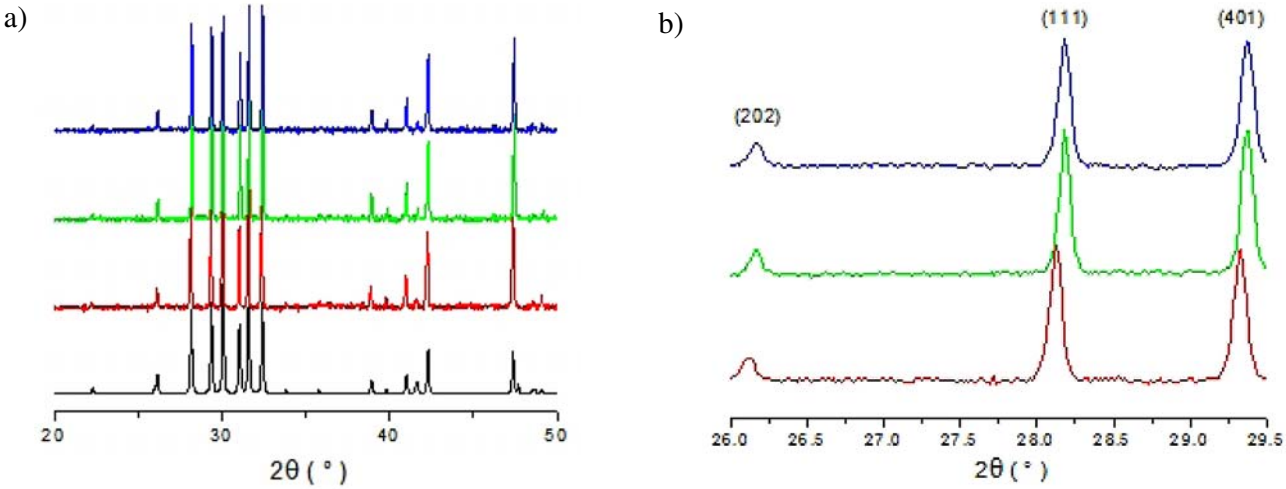

Figure 1: (a) XRD patterns of referenced Gd_2O_3 (PDF # 042–1465) (black), non-doped sintered Gd_2O_3 (red), as-synthesized monoclinic Gd_2O_3:Er,Yb (green) and sintered monoclinic Gd_2O_3:Er,Yb (blue), (b) XRD patterns in the narrower 2θ region with included three selected peaks corresponding to the marked *hkl* plane.

Table 1. d_{hkl}-values and the unit cell parameters of non-doped Gd_2O_3 and as-synthesized Er-,Yb-doped Gd_2O_3 products.

product	***d*-values (Å)**			**unit cell dimensions**				
monoclinic	d_{202}	d_{110}	d_{401}	***a* (Å)**	***b* (Å)**	***c* (Å)**	**β (°)**	***V* (Å^3)**
non-doped Gd_2O_3	3.410	3.170	3.043	14.110(3)	3.580(1)	8.773(2)	100.139(5)	436.17
Gd_2O_3:Er,Yb	3.404	3.164	3.038	14.100(4)	3.575(3)	8.766(4)	100.155(7)	434.98
cubic	d_{211}	d_{222}	d_{400}	***a* (Å)**	***V* (Å^3)**			
non-doped Gd_2O_3	4.420	3.122	2.704	10.8164(3)	1265.45			
Gd_2O_3:Er,Yb	4.411	3.119	2.701	10.8074(2)	1262.29			

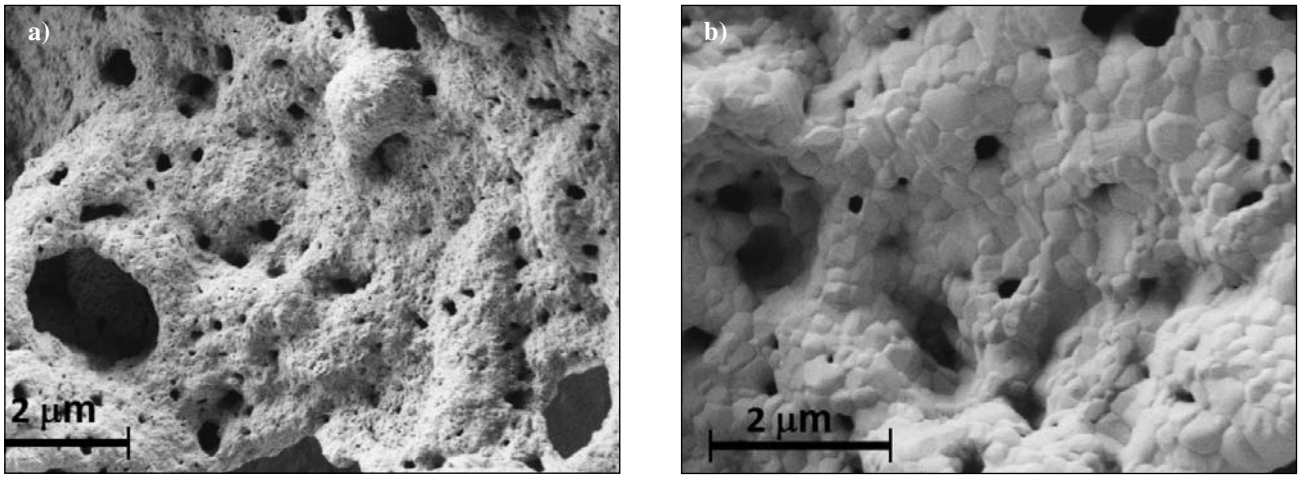

Figure 2. SEM micrographs of (a) as-synthesized and (b) sintered monoclinic Gd_2O_3:Er,Yb.

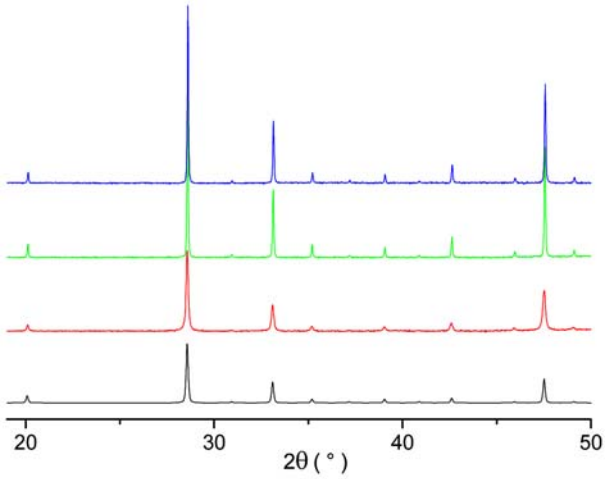

Figure 3. XRD patterns of referenced Gd_2O_3 (PDF # 012–0797) (black), non-doped sintered Gd_2O_3 (red), as-synthesized cubic Gd_2O_3:Er,Yb (green) and sintered cubic Gd_2O_3:Er,Yb (blue).

remains more or less the same but the faces of individual crystallites becomes more defined (see Figure 4b).

The crystallization of Gd_2O_3:Er,Yb is obviously governed by the temperature of pyrolisis process as it was already shown by Goldys et al.[20] Lower synthesis temperatures (up to 1300 °C) leads preferably to the formation of cubic phase, whereas higher synthesis temperatures result the crystallization of monoclinic phase. The temperature of the pyrolisis, however, is hard to control due to the large exothermic effect of the combustion reaction which often leads to the formation of non-pure Gd_2O_3 products affecting the luminescent properties of the material. We showed that the presence of different type of organic fuels in the reaction mixture can govern the temperature of combustion and consequently directs the formation of Gd_2O_3 phase. The combustion of reaction mixture containing only urea as an organic fuel is slower and non-intensive and leads to the formation of pure cubic Gd_2O_3:Er,Yb. The additional presence of β-alanine, on the other hand, causes vigorous exothermic reaction, where the temperature of combustion is clearly much higher than in the case of the synthesis containing only urea. This process yields the crystallization of phase pure monoclinic Gd_2O_3:Er,Yb. Note that the actual temperature of the com-

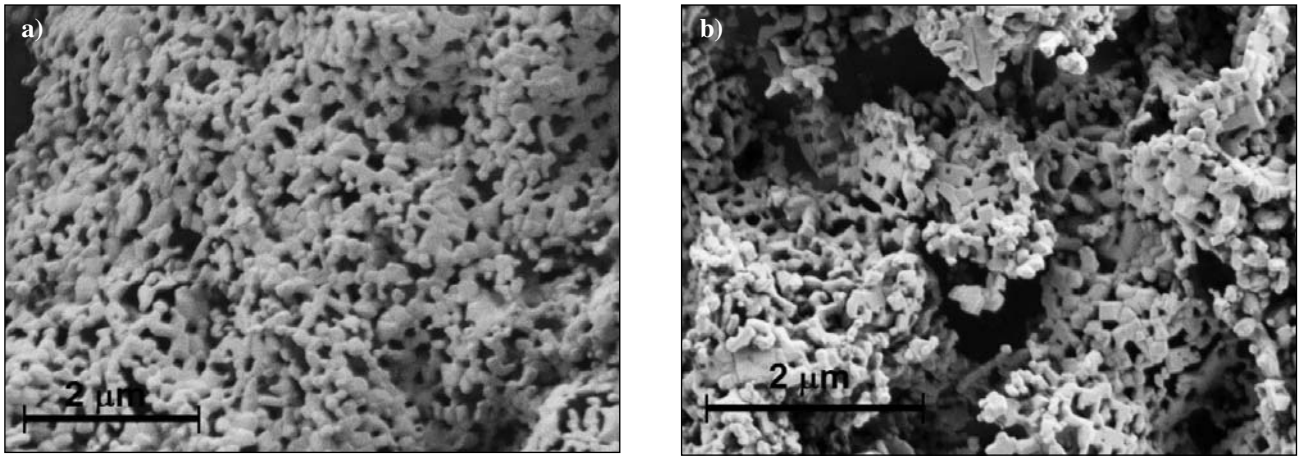

Figure 4. SEM micrographs of (a) as-synthesized and (b) sintered cubic Gd_2O_3:Er,Yb.

bustion is in both cases of synthesis procedures impossible to monitor, since the respond of probe cannot follow very fast temperature changes during the reaction.

3. 2. Upconversion Properties

The upconversion spectra of sintered Gd_2O_3:Er,Yb materials with cubic and monoclinic crystal system excited at 980 nm are shown in Figure 5. In both materials green and red upconverted emissions are shown. Absorption bands in relatively complex upconversion spectra caused by photon transitions via excited state absorption mechanism can be sorted in three groups. Er^{3+} and Yb^{3+} cations are promoted to the excited intermediate state in $^4I_{11/2}$ level and are subsequently raised to $^4F_{7/2}$ level by incoming pump photon. From this energy level, non-radiative decays to different lower states occur ($^2H_{11/2}$, $^4S_{3/2}$, $^4F_{9/2}$). First group of upconversion maxima between 520 and 540 nm is attributed to relaxation from $^2H_{11/2}$ to $^4I_{15/2}$ ground state. Second group of absorption bands occur between 540 and 570 nm due to the $^4S_{3/2} \rightarrow {}^4I_{15/2}$ transition and third group of upconversion maxima between 640 and 700 nm is attributed to the ground state relaxation from $^4F_{9/2}$ level.[16–19,21] The comparison of upconversion spectra belonging to cubic and monoclinic Gd_2O_3:Er,Yb shows that absorption maxima occur at approximately the same wavelengths, however the shapes of the spectra somewhat differ. Spectrum of cubic Gd_2O_3:Er,Yb shows distinctive and well defined maxima at 525, 537, 551 and 561 attributed to $^2H_{11/2} \rightarrow {}^4I_{15/2}$ and $^4S_{3/2} \rightarrow {}^4I_{15/2}$ transitions whereas absorption maxima in spectrum of monoclinic phase in the mentioned region are broad, less defined and split into several additional maxima. The splitting of the spectrum indicates polycrystalline nature of monoclinic Gd_2O_3:Er,Yb product and it is also related to the crystal symmetry features. In Gd_2O_3 with *C2/m* monoclinic system doped Er^{3+} and Yb^{3+} cations are in seven fold coordination and occupy three nonequivalent sites with C_s symmetry all contributing to the emission.[22] Similarly, the absence of splitting in cubic (*Ia-3*) Gd_2O_3 can also be explained by crystal structure features. In this case Er^{3+} and Yb^{3+} cations occur in six fold coordination and possess two crystallographically nonequivalent sites with C_2 and S_6 symmetries, respectively.[23] 75% of cations occupy C_2 sites, and 25% occupy S_6 sites. It is expected that mostly C_2 sites with higher occupancy contribute to the emission, resulting the absence of splitting in the upconversion spectra.

The intensities of the upconversion fluorescence bands of sintered monoclinic and cubic Gd_2O_3:Er,Yb were also monitored as a function of the temperature. We monitored intensity ratios of the bands at belonging to $^2H_{11/2} \rightarrow {}^4I_{15/2}$ and $^4S_{3/2} \rightarrow {}^4I_{15/2}$ transitions during the heating. The upconversion maxima of $^2H_{11/2} \rightarrow {}^4I_{15/2}$ transitions occur at 525 nm for both Gd_2O_3:Er,Yb phases, whereas bands corresponding to $^4S_{3/2} \rightarrow {}^4I_{15/2}$ transitions occur

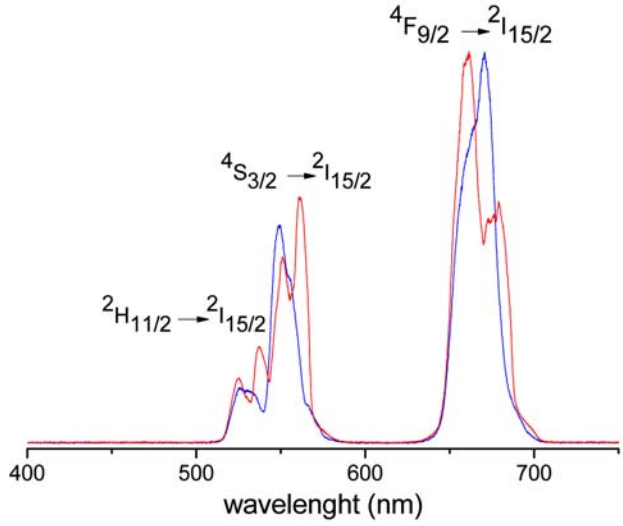

Figure 5. Green emission upconversion spectra of monoclinic (blue) and cubic (red) sintered Gd_2O_3:Er,Yb.

at 549 nm and 560 nm for monoclinic and cubic products, respectively. The energy difference between two excited states $^2H_{11/2}$ and $^4S_{3/2}$ is small and those two levels are thermally coupled. The band positions at 525 and 549 or 560 nm remain at the same wavelengths during the heating, however the band intensity ratios are strongly dependent on the temperature. The intensities of the absorption maxima at 525 nm are increasing whereas intensities of absorption maxima at 549 nm are gradually decreasing with temperature. As can be seen in Figure 6, the I_{525}/I_{549} or I_{525}/I_{560} intensity ratios obtained from spectra of monoclinic and cubic Gd_2O_3:Er,Yb products respectively show nearly linear temperature dependence in the broad temperature range. Even though cubic Gd_2O_3:Er,Yb show somewhat higher sensitivity for temperature changes, both materials can be used as upconversion temperature sensors in the range up to at least 300 °C.

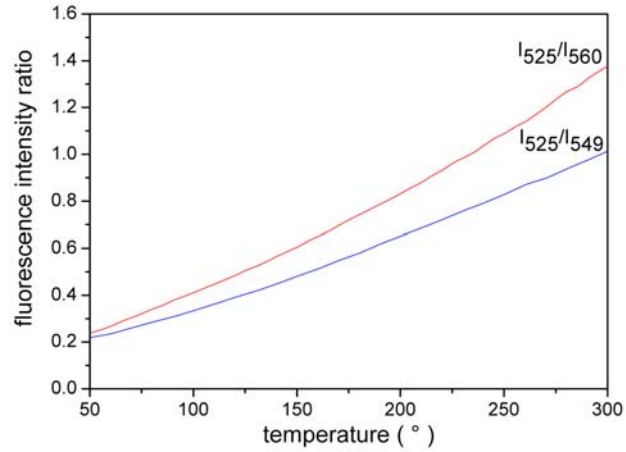

Figure 6. Fluorescence intensitiy ratios as a function of temperature of monoclinic (blue) and cubic (red) sintered Gd_2O_3:Er,Yb.

4. Conclusions

The Gd_2O_3:Er,Yb nanopowders with the Er^{3+}/Gd^{3+} and Yb^{3+}/Gd^{3+} molar ratios of 0.05 and 0.01 respectively were synthesized by combustion method. We showed that the combustion temperature can be effectively tuned by modification of organic fuel within reaction mixture which yields the crystallization of different Gd_2O_3 polymorphs. The presence of only urea used as organic fuel leads to low temperature combustion process yielding cubic Gd_2O_3:Er,Yb with high crystallinity and phase purity. The presence of additional β-alanine significantly increases the temperature of combustion yielding pure and highly crystalline Gd_2O_3:Er,Yb with monoclinic symmetry. The products were subsequently sintered at 1300 °C. The effective doping of Er^{3+} and Yb^{3+} cations within Gd_2O_3 was confirmed by XRD analysis. The change of morphologies and particle sizes after sintering process were observed by SEM analysis.

The influence of Gd_2O_3 structures on optical properties was evaluated by emission-excitation fluorescence measurements. Both, monoclinic and cubic polymorphs show similar upconversion effect with the spectral bands occurring at the same wavelengths, but the shape of spectra and intensity of individual bands differ. Both phases show strong temperature dependence of fluorescence intensity ratios (I_{525}/I_{549} and I_{525}/I_{560} for monoclinic and cubic polymorphs, respectively) belonging to $^2H_{11/2} \rightarrow {}^4I_{15/2}$ and $^4S_{3/2} \rightarrow {}^4I_{15/2}$ transitions. Although cubic Gd_2O_3:Er,Yb show somewhat higher sensitivity to heating than monoclinic polymorph, it was proven that both products can be applied for the temperature sensor devices based on upconversion intensity ratio changes in the range from room temperature to at least 300 °C.

5. References

1. W. O. Gordon, J. A. Carter, B. M. Tissue, *J. Lumin.* **2004**, *108*, 339–342.
2. D. Dosev, M. Nichkova, M. Liu, B. Guo, G. Liu, B. D. Hammock, I. M. Kennedy, *J. Biomed. Opt.* **2006**, *10*, 064006.
3. C. Feldmann, T. Justel, C. R. Ronda, P. J. Schmidt, *Adv. Funct. Mater.* **2003**, *13*, 511–516.
4. T. Igarashi, M. Ihara, T. Kusunoki, K. Ohno, T. Isobe, M. Senna, *Appl. Phys. Lett.* **2000**, *76*, 1549–1551.
5. P. Müller, M. Wermuth, H.U. Gudel, *Chem. Phys. Lett.* **1998**, *290*, 105–111.
6. X. Wang, X. Sun, D. Yu, B. Zou, Y. Li, *Adv. Mater.* **2003**, *15*, 1442–1445.
7. H. Song, B. Sun, T. Wang, S. Lu, L. Yang, B. Chen, X. Wang, X. Kong, *Solid State Commun.* **2004**, *132,* 409–413.
8. J. Hao, S. A. Studenikin, M. Cocivera, *J. Lumin.* **2001**, *93*, 313–319.
9. C.-C. Huang, C.-H. Su, W.-M. Li, T.-Y. Liu, Y.-H. Chen, C.-S. Yeh, *Adv. Funct. Mater.* **2009**, *19,* 249–258.
10. G. K. Das, B. C. Heng, S. C. Ng, T. White, J. S. C. Loo, L. D'Silva, P. Padmanabhan, K. K. Bhakoo, S. TamilSelvan, T. T. Y. Tan, *Lanmguir* **2010**, *26*, 8959–8965.
11. G. Tian, Z. Gu, X. Liu, L. Zhou, W. Yin, L. Yan, S. Jin, W. Ren, G. Xing, S. Li, Y. Zhao, *J. Phys. Chem. C* **2011**, *115*, 23790–23796.
12. D. K. Chatterjee, M.K. Gnanasammandhan, Y. Zhang, *Small*, **2010**, *6*, 2781–2795.
13. Z. Q. Li, Y. Zhang, *Angew. Chem. Int. Ed.* **2006**, *45*, 7732–7735.
14. S. Georgescu, V. Lupei, A. Petraru, C. Hapenciuc, C. Florea, C. Naud, C. Porte, *J. Lumin.* **2001**, *93*, 281–292.
15. A. Patra, C. S. Friend, R. Kapoor, P. N. Prasad, *J. Phys. Chem. B* **2002**, 106, 1909–1912.
16. S. K. Singh, K. Kumar, R. B. Rai, *Sensors Actuat. A* **2009**, *149*, 16–20.
17. W. Kong, J. Shan, Y. Ju, *Mater. Lett.* **2010**, *64*, 688–691.
18. S. K. Singh, K. Kumar, R. B. Rai, *J. Appl. Phys.* **2009**, *106*, 093520.
19. S. K. Singh, K. Kumar, R. B. Rai, *Appl. Phys. B* **2010**, *100*, 443–446.
20. E. M. Goldys, K. Drozdowicz-Tomsia, S. Jinjun, D. Dosev, I. M. Kennedy, S. Yatsunenko, M. Godlewski, *J. Am. Chem. Soc.* **2006**, *128*, 14498–14505.
21. F. Mangiarini, R. Naccache, A. Speghini, M. Battinelli, F. Vetrone, J. A. Capobianco, *Mater. Res. Bull.* **2010**, *45*, 927–932.
22. J. Hölsä, T. Leskelä, M. Leskelä, *Inorg. Chem.* **1988**, *24*, 1539–1542.
23. E. Antic-Fidancev, J. Hölsä, M. Lastusaari, *J. Phys. Condens. Matter.* **2003**, *15*, 863–876.

Povzetek

Nanokristalinični Gd_2O_3 produkti dopirani z Er^{3+} in Yb^{3+} kationi so bili pripravljeni z izgorevalno sintezo. Pokazali smo, da lahko temperaturo izgorevanja kontroliramo s prisotnostjo organskih gorivnih dodatkov v reakcijskih zmeseh. Izgorevanje poteka pri nižjih temperaturah v prisotnosti uree, kar vodi do kristalizacije kubične Gd_2O_3:Er,Yb faze, medtem ko dodatna prisotnost β-alanina poleg uree povzroči izgorevanje pri višji temperaturi in s tem do kristalizacije monoklinskega Gd_2O_3:Er,Yb polimorfa. Učinkovito dopiranje Er^{3+} in Yb^{3+} v Gd_2O_3 je bilo potrjeno z XRD analizo. Oba dopirana polimorfa kažeta nadkonverziji v zelenem in redečem območju vidne svetlobe. Močna odvisnost razmerja fluorescenčnih intenzitet (I_{525}/I_{549} za monoklinski in I_{525}/I_{560} za kubični polimorf) od temperature pa kaže na uporabnost obeh faz v temperaturnih senzorskih napravah, ki delujejo na osnovi spremembe nadkonverzijskih intenzitet.